ARTICLE   OPEN

Check for updates

PvDBPII elicits multiple antibody-mediated mechanisms that reduce growth in a *Plasmodium vivax* challenge trial

Francisco J. Martinez [1], Michael White[2], Micheline Guillotte-Blisnick[1], Christèle Huon[1], Alix Boucharlat[3], Fabrice Agou[3], Patrick England [4], Jean Popovici[5], Mimi M. Hou[6,7,8], Sarah E. Silk[6,7,8], Jordan R. Barrett[6,7,8], Carolyn M. Nielsen[6,7,8], Jenny M. Reimer [9], Paushali Mukherjee[10], Virander S. Chauhan [11], Angela M. Minassian[6,7,8,12], Simon J. Draper [6,7,8,12] and Chetan E. Chitnis[1 ✉]

The receptor-binding domain, region II, of the *Plasmodium vivax* Duffy binding protein (PvDBPII) binds the Duffy antigen on the reticulocyte surface to mediate invasion. A heterologous vaccine challenge trial recently showed that a delayed dosing regimen with recombinant PvDBPII SalI variant formulated with adjuvant Matrix-M™ reduced the in vivo parasite multiplication rate (PMR) in immunized volunteers challenged with the Thai *P. vivax* isolate PvW1. Here, we describe extensive analysis of the polyfunctional antibody responses elicited by PvDBPII immunization and identify immune correlates for PMR reduction. A classification algorithm identified antibody features that significantly contribute to PMR reduction. These included antibody titre, receptor-binding inhibitory titre, dissociation constant of the PvDBPII-antibody interaction, complement C1q and Fc gamma receptor binding and specific IgG subclasses. These data suggest that multiple immune mechanisms elicited by PvDBPII immunization are likely to be associated with protection and the immune correlates identified could guide the development of an effective vaccine for *P. vivax* malaria. Importantly, all the polyfunctional antibody features that correlated with protection cross-reacted with both PvDBPII SalI and PvW1 variants, suggesting that immunization with PvDBPII should protect against diverse *P. vivax* isolates.

INTRODUCTION

Plasmodium vivax accounts for majority of malaria cases outside sub-Saharan Africa, where *P. falciparum* is more predominant[1]. For many decades, *P. vivax* malaria was considered to be a 'benign' infection. However, recent studies have reported significant incidence of severe symptoms in *P. vivax* malaria[2,3]. Ineffective control of *P. vivax* could pose an important public health threat to communities in which *P. vivax* is endemic or at risk of emerging. Current efforts to control malaria are less effective in reducing *P. vivax* compared to *P. falciparum* due to the unique biology of *P. vivax*[4]. For example, the dormant liver stage of *P. vivax* known as the hypnozoite can reactivate and cause blood stage infection weeks, months or even years after the initial infection. This dormant stage, which cannot be detected, greatly contributes to *P. vivax* prevalence[5]. In addition, *P. vivax* gametocytes appear early in the blood stage, so the parasite can be transmitted even before the first symptoms appear and treatment is administered to the patient[6]. An effective vaccine that can prevent *P. vivax* infection, reduce blood stage replication and protect against disease could greatly help efforts to control and eventually eliminate *P. vivax*.

During the blood stage, the invasive form of *P. vivax* known as the merozoite repeatedly infects and multiplies within reticulocytes causing the clinical symptoms of malaria. The invasion of reticulocytes is mediated by the interaction of the *P. vivax* Duffy binding protein (PvDBP) and the Duffy antigen receptor for chemokines (DARC)[7,8]. The amino-terminal cysteine-rich region II

of PvDBP (PvDBPII), serves as the binding domain of this invasion ligand[9]. Importantly, Duffy-negative individuals remain largely resistant to *P. vivax* infection[7]. Numerous reports indicate PvDBPII is highly polymorphic[10–12], suggesting that it is under intense immune pressure. However, the binding residues in PvDBPII that make contact with DARC are highly conserved[13–15]. The binding residues, which include positively charged as well as hydrophobic amino acids, assemble on the PvDBPII surface to form a receptor recognition site that is fully exposed to neutralization by antibodies[15]. Moreover, since the binding residues are conserved, antibodies that target them are predicted to be strain-transcending and capable of neutralizing diverse *P. vivax* strains. Indeed, upon natural exposure a small percentage of individuals develop high titre binding inhibition antibodies against PvDBPII that are cross-reactive[16,17]. Importantly, the presence of such high titre binding inhibitory antibodies against PvDBPII is associated with reduced risk of *P. vivax* infection[16,17]. However, the low frequency of individuals in the population with such binding inhibitory antibodies indicates that natural exposure is not effective at eliciting protective anti-PvDBPII antibodies.

Pre-clinical studies demonstrated that immunization of animals with recombinant PvDBPII readily elicits high titre binding inhibitory antibodies that cross-react with multiple variants[18,19]. A vaccine based on PvDBPII could thus potentially elicit binding inhibitory antibodies that limit blood-stage growth of diverse *P. vivax* isolates. To date, two delivery platforms developed for

PvDBPII have been tested in clinical trials. These include recombinant PvDBPII protein formulated with adjuvants such as glucopyranosyl lipid adjuvant-stable emulsion (GLA-SE)[20] and PvDBPII delivered by two viral vectors, namely, replication-deficient chimpanzee adenovirus serotype 63 (ChAd63) for priming followed by modified vaccinia virus Ankara (MVA) for boosting[21]. The vaccine candidate PvDBPII/GLA-SE was shown to be safe and no related adverse events were associated with the vaccine[20]. In addition, PvDBPII-specific antibodies were elicited and shown to inhibit DARC-binding by diverse PvDBPII variants[20]. In a Phase I trial with UK adult volunteers, the viral-vectored PvDBPII showed similar safety and immunogenicity results[21]. Recently, PvDBPII protein reformulated in Matrix-M[TM] adjuvant (PvDBPII/Matrix-M[TM]) from Novavax, and PvDBPII expressed by the same viral vectors, ChAd63/MVA, were tested in parallel in a Phase I/IIa blood stage challenge clinical trial using a heterologous *P. vivax* isolate to evaluate efficacy[22]. Interestingly, volunteers who were vaccinated with PvDBPII/Matrix-M[TM] in a delayed dosing schedule showed significant reduction in the parasite multiplication rate (PMR) compared to unvaccinated volunteers. None of the other groups in the trial, including PvDBPII delivered by viral vectors, showed any reduction in PMR. This result provided proof-of-concept that immunization with PvDBPII can elicit immune responses that can impair in vivo growth of a heterologous *P. vivax* strain. Here, we report extended analyses of the antibody responses, including functional analysis of anti-PvDBPII antibodies, PvDBPII-antibody binding kinetics, recognition of native PvDBP in *P. vivax* schizonts as well as binding to C1q and Fc gamma receptors, to identify immune correlates of protection following immunization with vaccine candidates based on PvDBPII.

RESULTS

Functional analysis of antibody response to PvDBPII in a challenge trial

A schematic describing the challenge trials to evaluate efficacy of PvDBPII administered using two approaches for vaccine antigen delivery, namely, recombinant PvDBPII SalI protein adjuvanted with Matrix-M[TM], PvDBPII/Matrix-M[TM], and PvDBPII SalI delivered by viral-vectors, ChAd63 followed by MVA (ChAd63/PvDBPII and MVA/PvDBPII)[22] is shown in Supplementary Fig. 1.

As described earlier[22], volunteers received priming immunizations with PvDBPII/Matrix-M[TM] and ChAd63/PvDBPII in January 2020. The trial was halted in March 2020 due to the Covid-19 pandemic. Twelve volunteers in the PvDBPII/Matrix-M[TM] arm ($n = 12$) received the priming dose and one booster dose of PvDBPII/Matrix-M[TM] at 1 month, whereas ten volunteers from the viral vectors arm ($n = 10$) had only received the priming dose of ChAd63/PvDBPII by the time the trial was put on halt in March 2020. The trial was restarted in April 2021 by which time several volunteers had dropped out of the trial. Six volunteers who received the first 2 monthly doses of the recombinant PvDBPII/Matrix-M[TM] in January and February 2020 (days 0 and 28), got the final boost after 14 months (day 440) and underwent Controlled Human Malaria Infection (CHMI) with *P. vivax* blood-stage parasites (clonal strain PvW1)[23] in May 2021. We refer to this group as PvDBPII/M-M (0-1-14 months). Two volunteers, who received the ChAd63/PvDBPII prime in January 2020 (day 0), received an additional ChAd63/PvDBPII followed by MVA/PvDBPII at 17 and 19 months (days 530 and 586), respectively. We designated this group as VV-PvDBPII (0-17-19 months). New volunteers were enrolled in the trial and four of them received PvDBPII/Matrix-M[TM] in a regimen of 0, 1 and 2 months (days 530, 558 and 586) and three others received ChAd63/PvDBPII followed by MVA/PvDBPII scheduled at 0 and 2 months (days 530 and 586). These short regimen groups (with vaccines given as originally intended) are referred to as groups PvDBPII/M-M (0-1-2 months)

and VV-PvDBPII (0–2 months), respectively. Volunteers from PvDBPII/M-M (0-1-2 months), VV-PvDBPII (0-17-19 months) and VV-PvDBPII (0–2 months) groups underwent CHMI in October 2021. Regardless of the vaccine regimen, all volunteers underwent CHMI 2–4 weeks after the last immunization. Seven individuals who did not received any vaccine were included as the control group in the CHMI conducted in May 2021 and four nonvaccinated volunteers underwent CHMI in October 2021 (infectivity controls). Both CHMI challenges involved infection with blood-stage parasites of the heterologous *P. vivax* monoallelic isolate W1 (or PvW1)[23]. Parasite growth was evaluated in immunized and control unvaccinated groups by RT-PCR at different time points during the CHMI to determine vaccine efficacy[22].

As reported earlier[22], only the PvDBPII/M-M (0-1-14 months) group showed a significant reduction of the PMR compared to infectivity controls (median PMR of 3.2 for PvDBPII/M-M (0-1-14 months) group and median PMR of 6.8 for controls, $p = 0.002$). This represented a 53% reduction of the median PMR in PvDBPII/M-M (0-1-14 months) group compared to controls. No other vaccine group had a significant impact on the PMR. The PMR data from the challenge trial[22] is summarized for clarity in Table 1.
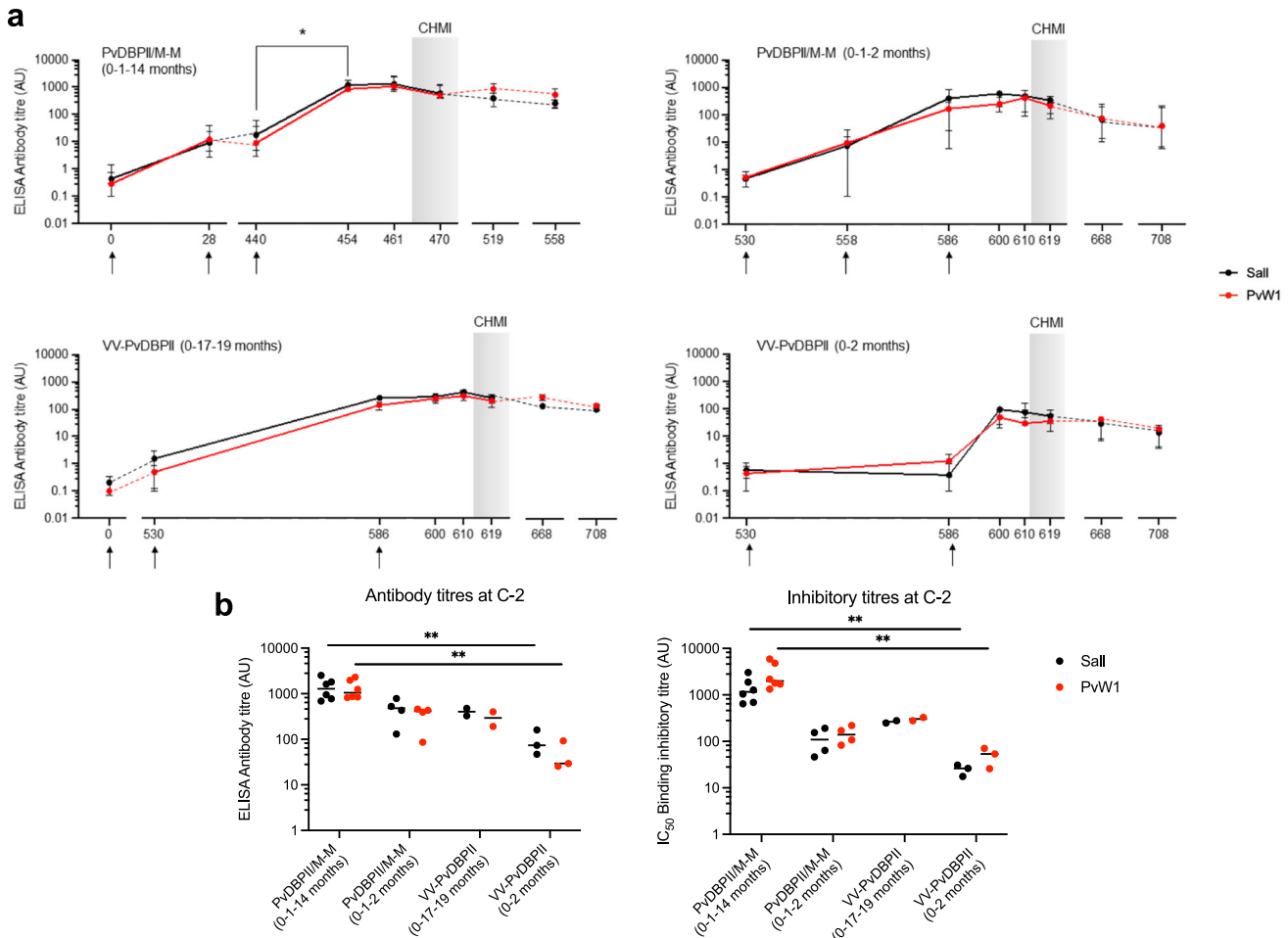
ELISA titres for recognition of the homologous PvDBPII SalI domain and PvW1 (the heterologous PvDBPII domain from the *P. vivax* strain used for CHMI) by sera from immunized volunteers were determined through the course of the trial (Fig. 1a). Anti-PvDBPII antibody titres peaked 2 weeks after final boost in all vaccinated volunteers. The antibody titres of sera in the PvDBPII/M-M (0-1-14 months) group increased significantly after the delayed second boost at day 440 for both PvDBPII SalI and PvW1. In case of PvDBPII/M-M (0-1-2 months), VV-PvDBPII (0-17-19 months) and VV-PvDBPII (0–2 months) groups, there was no significant increase after the second monthly boost. The anti-PvDBPII antibody titres in group PvDBPII/M-M (0-1-14 months), which was the only group to show a significant PMR reduction, remained stable after second boost and challenge with only a marginal decline over a 4-month period after the delayed second boost (Fig. 1a). In the groups immunized with viral-vectored PvDBPII, the anti-PvDBPII antibodies reached a peak after MVA boost prior to challenge (Fig. 1a).

Next, we compared the antibody responses at C-2, 2 days before challenge, against PvDBPII SalI and PvW1. Sera from the immunized volunteers had similar ELISA recognition titres for PvDBPII SalI and PvW1 in all the groups (Fig. 1b). Also, at C-2, the antibody titres of group PvDBPII/M-M (0-1-14 months) for recognition of PvDBPII were not significantly different from titres of groups PvDBPII/M-M (0-1-2 months) or VV-PvDBPII (0-17-19 months) for either PvDBPII SalI or PvW1. The only statistically significant differences were found for antibody titres for recognition of both PvDBPII SalI and PvW1 between groups PvDBPII/M-M

Table 1. In vivo parasite multiplication rate (PMR) of vaccinated groups and controls following blood stage challenge with *P. vivax* PvW1.

Group	No of volunteers	Median PMR	Range
PvDBPII/M-M (0-1-14 months)	6	3.2 (**)	2.3–4.3
PvDBPII/M-M (0-1-2 months)	4	6.3 (ns)	5.1–7.9
VV-PvDBPII (0-17-19 months)	2	5.8 (ns)	4.9–6.8
VV-PvDBPII (0–2 months)	3	5.8 (ns)	4.4–5.8
Infectivity controls	11	6.8	4.0–7.8

Median and p values are reported, ** $p < 0.01$, Krustal-Wallis test with Dunn's correction for multiple comparisons.

Fig. 1 ELISA reactivity and binding inhibitory activity of sera from volunteers after immunization with protein-in-adjuvant or viral-vectored PvDBPII vaccines. a ELISA titres for recognition of PvDBPII SalI by sera from volunteers at different timepoints over the course of the trial reported as median and range for each vaccine group are shown. Black arrows show the time points of the immunizations. Shaded grey areas represent the period after blood stage *P. vivax* challenge. **b** ELISA recognition titres and binding inhibition titres for PvDBPII variants SalI and PvW1 for all volunteers at C-2. Medians are shown in horizontal bars, **$p < 0.01$, Kruskal–Wallis test with Dunn's correction for multiple comparisons.

(0-1-14 months) and VV-PvDBPII (0–2 months) (Fig. 1b). Control sera from volunteers that did not receive any immunization were seronegative for recognition of PvDBPII SalI and PvW1 (arbitrary units, AU ≤ 1) at all time points including C-2.

We also assessed the ability of anti-PvDBPII sera to block DARC-receptor binding by PvDBPII SalI and PvW1. Sera from infectivity controls at C-2 and day 0 sera from volunteers collected prior to immunization showed DARC-binding inhibition of ≤30% for PvDBPII SalI and PvW1 at the lowest serum dilution of 1:10 that was tested in the binding inhibition assay. Binding inhibition for all vaccine groups at C-2 tested at 1:10 dilution was greater >90%. Anti-sera of PvDBPII/M-M (0-1-14 months) group with delayed boost of PvDBPII/Matrix-M™ tended to have the highest binding inhibition titres at C-2 (Fig. 1b). However, only comparison between PvDBPII/M-M (0-1-14 months) and VV-PvDBPII (0–2 months) reached statistical significance. There was no difference in binding inhibition titres for PvDBPII SalI and PvW1 in all vaccinated groups at C-2.

In order to examine the stability of anti-PvDBPII antibodies, we analyzed correlations in antibody recognition titres and binding inhibition titres at time points C-2, C + 56 and C + 96 (Supplementary Fig. 2). The antibody recognition titres and binding inhibition titers were highly correlated between time points C-2 and C + 56 or C + 96.

PvDBPII-specific antibodies recognize native antigen in *P. vivax* schizonts

The ability of anti-PvDBPII sera to recognize native PvDBP in *P. vivax* schizonts was determined by IFA. All sera from vaccinated volunteers collected on day C-2 showed apical staining in merozoites within mature *P. vivax* schizonts (Fig. 2a). Day 0 control sera collected prior to immunization (D0) did not show any specific signal in IFA with *P. vivax* schizonts (Fig. 2a). Sera collected at C-2 from the PvDBPII/M-M (0-1-14 months) group had the highest reactivity at dilutions of 1:500 and 1:5,000 (Fig. 2b). Day C-2 sera from the VV-PvDBPII (0-17-19 months) group had higher signal than sera collected at C-2 from groups PvDBPII/M-M (0-1-2 months) and VV-PvDBPII (0-2 months) at dilution of 1:5,000. Sera at C-2 from PvDBPII/M-M (0-1-2 months) group had stronger reactivity than VV-PvDBPII (0-2 months) at 1:500 (Fig. 2b). Based on signal intensity, we can order the groups from highest to lowest serum reactivity in IFA as follows: PvDBPII/M-M (0-1-14 months) > VV-PvDBPII (0-17-19 months) > PvDBPII/M-M (0-1-2 months) > VV-PvDBPII (0-2 months).

Immune correlates for PMR reduction

To explore the immune processes that are associated with the PMR outcome, we measured diverse antibody functions and determined their correlation to PMR reduction calculated for each
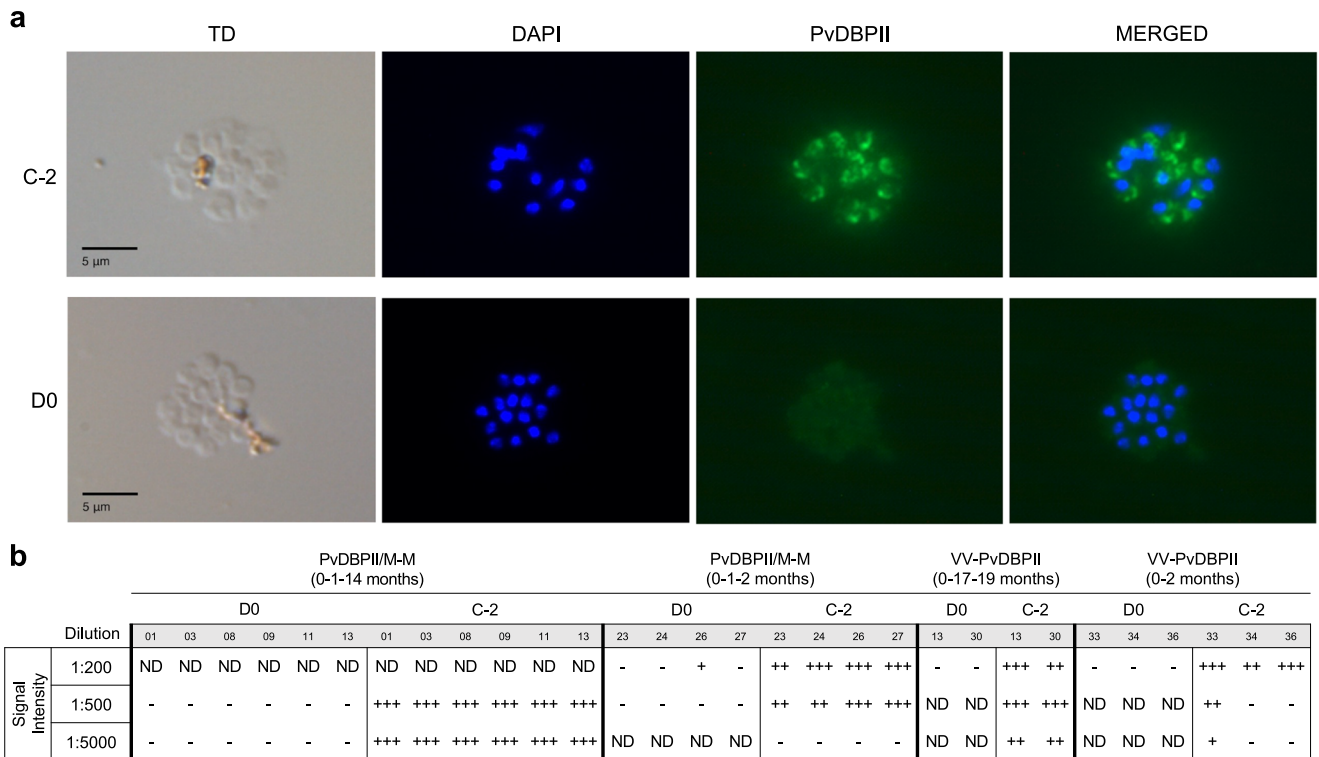
Fig. 2 Reactivity of sera from immunized volunteers with *P. vivax* schizonts. a Representative images of *P. vivax* schizonts incubated with sera from an individual of the PvDBPII/M-M (0-1-14 months) group at dilution 1:5000. Sera at time point C-2 showed apical staining to PvDBP (green) in *P. vivax* schizonts compared to sera collected prior to initial immunization (D0). **b** Signal intensity in IFA for day C-2 and D0 sera from different groups tested at different dilutions. The fluorescence intensity of each sample was scored as: +++, for high intensity; ++, medium intensity; +, low intensity; and -, no signal. Some IFA samples that were not done are designated as ND.

individual as: 100 − (test PMR x 100)/(PMR of unvaccinated controls). Multivariate analysis was performed with all the variables for both PvDBPII alleles SalI and PvW1 using a frequently-used machine learning tool, the classification algorithm Boruta[24], in order to select the features that significantly contribute to the PMR outcome and rank them according to their contribution or importance in predicting the PMR outcome.

Sera from timepoint C-2 was used to evaluate i) the PvDBPII-binding kinetics of the polyclonal antibodies (affinity, association and dissociation constants or K_D, k_a and k_{dis} respectively); ii) antibody isotypes and subclasses; iii) binding capacity for complement component C1q and Fc gamma receptors or FcγRs; iv) avidity; and v) ELISA recognition titres and binding inhibition titres for PvDBPII. Both datasets corresponding to either antibody functions specific to PvDBPII SalI (Fig. 3a) or to PvDBPII PvW1 (Fig. 3c) showed significant correlations between most of the variables. We observed positive correlations between C1q binding, FcγR binding, isotypes, antibody recognition titres and binding inhibition titres in both datasets (Fig. 3a, c). Negative correlations were observed for the affinity and dissociation constants, K_D and k_{dis}, in the PvDBPII SalI dataset (Fig. 3a), whereas all three PvDBPII-antibody binding kinetic constants in the PvDBPII PvW1 dataset showed negative correlations with the rest of the dataset (Fig. 3c). The IgG3 and IgM readouts did not show correlations to most of the features of both datasets (Fig. 3a, c).

PMR reduction showed a significant correlation in the PvDBPII SalI dataset with antibody recognition titre, binding inhibition titre, k_{dis}, IgG1, IgG2, IgG4, IgA, C1q binding and FcγR binding (Fig. 3a). In case of the PvDBPII PvW1 dataset, the PMR reduction showed significant correlations with the variables mentioned above for PvDBPII SalI dataset, K_D and avidity (Fig. 3c). We proceeded to identify the variables that have a significant contribution to the PMR reduction outcome in both datasets.

The Boruta algorithm selected as important the same 11 readouts in both datasets (Fig. 3b and d). These important variables include binding inhibition titres, FcγR binding and C1q binding, IgG1, IgG2, IgG4, k_{dis} and antibody titres. Binding inhibition titre appeared as the variable with the highest importance in the PvDBPII SalI dataset (Fig. 3b). In case of the PvDBPII PvW1 dataset, this variable also had high importance in the dataset (Fig. 3d). Correlations of the PvDBPII SalI and PvW1 binding inhibition titres to PMR reduction showed high significance ($p \le 0.0014$) (Fig. 4a). This feature was also highly correlated when both PvDBPII alleles were compared (Fig. 4b), indicating that immunization with PvDBPII SalI elicits antibodies that cross-react with PvDBPII PvW1. We modeled PMR reduction using a Random Forest regression with binding inhibition titres specific to the two PvDBPII alleles. The importance of the two features as a PMR reduction predictor was similar and no statistical difference was observed (Fig. 4c), indicating both binding inhibition titers specific to SalI and PvW1 contribute equally to predict the PMR outcome.

Correlations to PMR reduction for the rest of the variables considered as important by the Boruta algorithm in the PvDBPII SalI and PvW1 datasets are shown in Supplementary Figs. 3 and 4, respectively. All these correlations to PMR reduction were statistically significant (Supplementary Figs. 3 and 4). The unimportant variables of both datasets are also shown in Supplementary Figs. 5 and 6 (PvDBPII SalI and PvW1 datasets, respectively). In case of the variables specific to PvDBPII SalI, IgA was significantly correlated to PMR reduction but it was not considered as an important predictor by the Boruta algorithm (Supplementary Fig. 5). In case the variables specific to PvDBPII PvW1, avidity, K_D and IgA also correlated to the PMR reduction but they were not significant predictors as per the Boruta algorithm (Supplementary Fig. 6). Next, we compared individually the 10 variables selected as important by the Boruta algorithm between
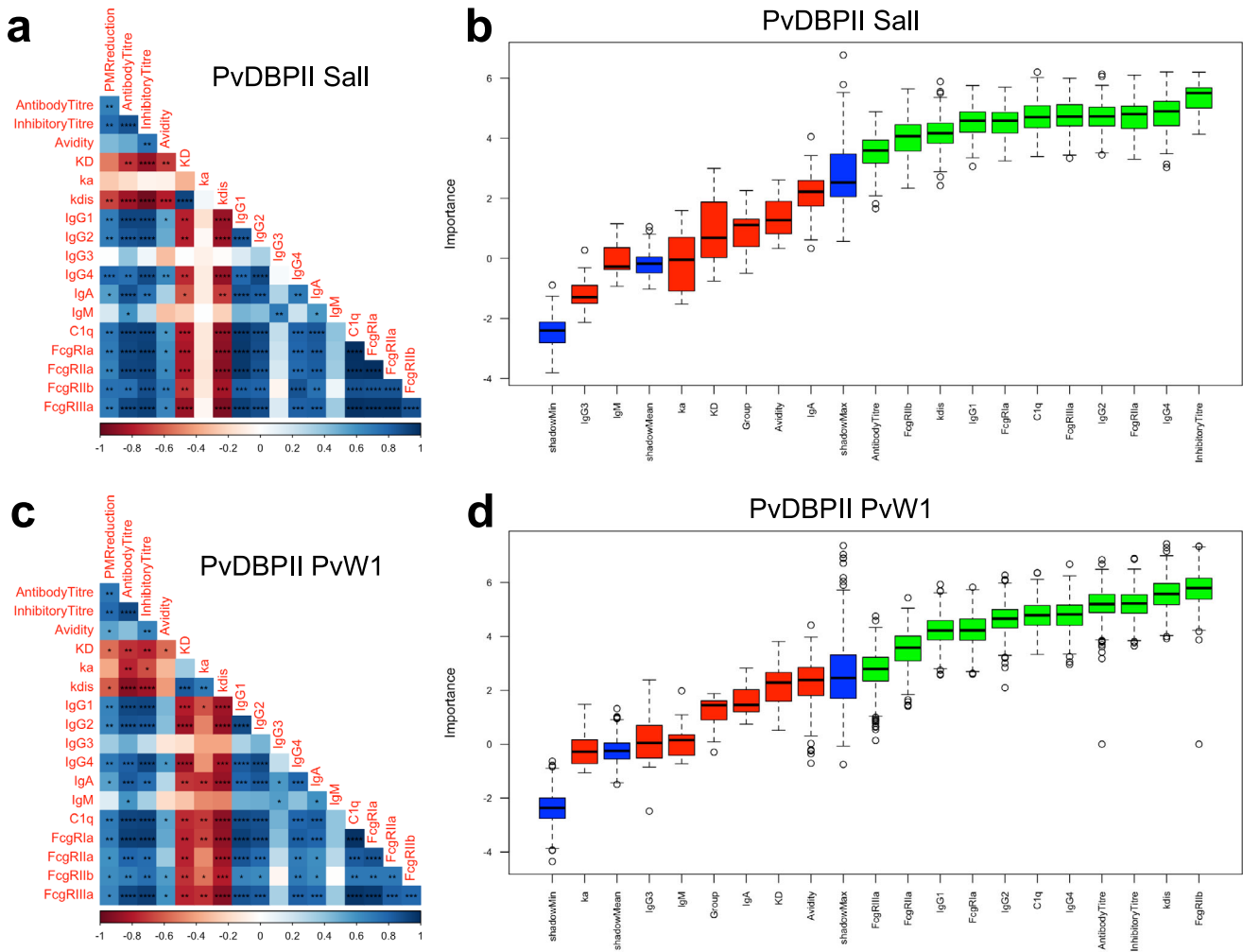
Fig. 3 Variable correlations and feature selection of the antibody functions measured in the study. a Correlations between the anti-PvDBPII Sall antibody functions are shown. Correlation coefficients (shown in a double red-blue gradient) for each comparison were calculated using Spearman's rank correlation tests. p values for each significant correlation are indicated, $*p < 0.05$ $**p < 0.01$ $***p < 0.001$ $****p < 0.0001$. **b** Importance plot for classification of variables specific to PvDBPII Sall that significantly contribute to the PMR reduction using the Boruta algorithm. The importance of each variable is defined as the Z-score of the mean decrease accuracy (normalised permutation importance). Blue boxes correspond to the minimal, average, and maximum Z-scores of shadow features. The variables that contribute significantly (green) or not (red) to the PMR reduction are shown. Boxplots show median Z-score (horizontal bar), interquartile range (boxes), range (whiskers), and outliers (open circles). **c** Correlations between the PvDBPII PvW1 antibody functions are depicted as in **a**. **d** Importance plot for classification of variables specific to PvDBPII PvW1 are depicted as in **b**.

the PvDBPII Sall and PvW1 datasets, with the exception of the binding inhibition titres, already shown in Fig. 4B. We observed significant correlations for all the variables ($p \leq 0.001$) (Supplementary Fig. 7), indicating strong cross-reactivity of polyfunctional PvDBPII-specific antibodies that correlate with PMR reduction.

DISCUSSION

Two vaccine platforms, recombinant protein-in-adjuvant and viral vectors were used to deliver the leading vivax malaria vaccine candidate PvDBPII to volunteers in a challenge trial to evaluate their efficacy[22]. A PMR reduction of 53% was observed in the volunteers who received PvDBPII/Matrix-M™ in a delayed dosing regimen of 0, 1 and 14 months, group PvDBPII/M-M (0-1-14 months)[22]. No impact on the PMR was found in groups that received PvDBPII/Matrix-M™ with monthly regimen of 0, 1 and 2 months or viral-vectored PvDBPII at 0 and 2 months or 0, 17 and 19 months, groups PvDBPII/M-M (0-1-2 months), VV-PvDBPII (0–2 months) and VV-PvDBPII (0-17-19 months), respectively[22]. Here, we performed exploratory analysis to evaluate the antibody

responses in vaccinated volunteers to identify immune correlates associated with PMR reduction.

All vaccinated volunteers seroconverted after immunizations with both vaccine platforms. Sera collected 2 days before challenge (day C-2) were analyzed for polyfunctional antibody responses. Day C-2 sera from the PvDBPII/M-M (0–1–14 months) group tended to have higher anti-PvDBPII recognition titres, binding inhibition titres and reactivity to native PvDBP in *P. vivax* schizonts by IFA compared to other groups. These findings are in accordance with studies showing improved antibody responses and neutralizing activity with delayed dosing regimens in vaccines targeting *P. falciparum* blood-stage antigen PfRH5[25,26] and SARS-Cov-2[27,28]. This improved immunogenicity in delayed dosing regimens may arise from increased B cell populations. Indeed, the exploratory analyses of the PvDBPII-specific cellular responses conducted in the volunteers of this trial showed that memory B cells (CD19 + CD27 + IgG+) and plasma cells (CD19 + CD27 + CD38+) were significantly higher in delayed dosing regimens 7 days after final boost with both vaccine platforms used here[29]. In addition, these two B cell populations
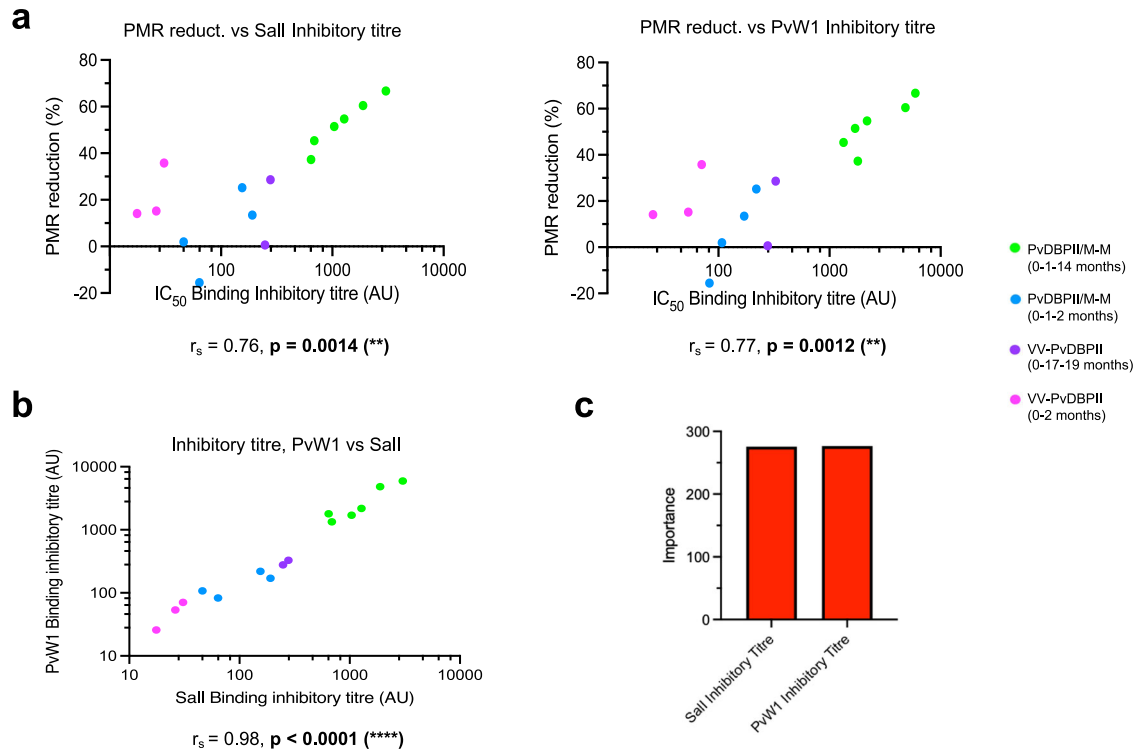
Fig. 4 Correlation of binding inhibition titre and PMR reduction. a Individual correlations of the PMR reduction and binding inhibition titres for PvDBPII SalI or PvW1. (**b**) Correlation between binding inhibition titres for PvDBPII SalI and PvW1. Correlations shown in **a** and **b** were calculated using Spearman's rank correlation tests. Correlation coefficients and p values for each comparison are shown. **c** Importance plot for the binding inhibition titres specific to PvDBPII SalI and PvW1 using Random Forest regression of the PMR reduction.

are significantly correlated to PMR reduction[29]. Extending the time between immunizations thus substantially improves antibody responses to PvDBPII potentially translating into greater efficacy.

The administration of the delayed dosing regimen of PvDBPII/ Matrix-M[TM] [PvDBPII/M-M (0-1-14 months) group] resulted in a PMR reduction of 53% compared to unvaccinated controls. To our knowledge, this PMR reduction is the highest observed for any blood-stage malaria vaccine tested in CHMI[25,30-34]. The highest PMR reduction observed in CHMI following immunization with a blood-stage antigen thus far was 17% for the *P. falciparum* blood-stage antigen, PfRH5[25]. Immunization with other *P. falciparum* blood-stage antigens such as PfMSP1$_{42}$ and PfAMA1 did not elicit significant parasite growth inhibition in vivo[30-34]. A malaria vaccine should protect against infection by diverse strains. Immunization with the PvDBPII SalI variant elicits cross-reactive antibodies capable of inhibiting DARC-binding by multiple PvDBPII variants in pre-clinical[18,19] and clinical[20,21] studies. PvDBPII-specific antibodies inhibit binding to DARC by both PvDBPII alleles, SalI and PvW1, with similar efficiency (Fig. 1B). The essential residues of PvDBPII that bind to DARC are conserved in the highly divergent PvW1 sequence[13-15]. Additional analyses are required to determine if the binding inhibitory antibodies target these conserved DARC binding residues. If that is the case, we would expect that heterologous *P. vivax* parasites such as PvW1 would be as susceptible for growth inhibition as the homologous strain SalI. A challenge trial with homologous parasites would probably result in a similar PMR reduction as seen in this heterologous challenge trial[22]. Further trials involving heterologous and homologous *P. vivax* challenge strains will reveal the extent of the cross-reactive protection elicited by PvDBPII immunization.

The immune correlates of protection against *P. vivax* are not clearly defined. Here, in addition to determining antibody recognition and binding inhibition titres, we evaluated polyfunctional antibody responses elicited by PvDBPII SalI immunization to identify immune parameters that are associated with PMR reduction. We found that in addition to antibody recognition and binding inhibition titres, PMR reduction is correlated with k_{dis}, IgG1, IgG2, IgG4, IgA, C1q binding and FcγR binding for antibodies against both PvDBPII SalI and PvW1 variants (Fig. 3a, c). Using the Boruta classifying algorithm, we obtained the same 11 variables that significantly contribute to PMR reduction in both PvDBPII SalI and PvW1 datasets (Fig. 3b, d). Although a statistical analysis cannot definitively prove that a biomarker is causally associated with protection rather than just correlated, the variable that showed the highest importance in the PvDBPII SalI dataset was the binding inhibition titre (Fig. 3b), which also had high importance in the PvDBPII PvW1 dataset (Fig. 3d). The binding inhibition titres specific to the two PvDBPII variants were highly correlated (Fig. 4b) and modeled PMR reduction similarly when combined (Fig. 4c). This may indicate the significant value of PvDBPII-DARC binding inhibition titres as a *P. vivax* protection predictor. The high correlation between PvDBPII binding inhibition titres for SalI and PvW1 (Fig. 4b) reflects the cross-reactivity of these high titre binding inhibitory antibodies. Children residing in a malaria-endemic area of Papua New Guinea (PNG), who developed high-titre cross-reactive binding inhibitory antibodies to PvDBPII had a reduced risk of *P. vivax* infection and lower parasite densities[16]. However, the IC$_{50}$ binding inhibition titres of these naturally acquired antibodies was ~1:20[16]. In comparison, day C-2 sera of the PvDBPII/M-M (0-1-14 months) group showed 50-100 times higher binding inhibition titres with IC$_{50}$ of ~1:1000 to 1:2000 (Fig. 1b). Given that PvDBPII immunization elicits substantially higher binding inhibition titres compared to naturally acquired binding inhibitory antibodies that are associated with protection, one can expect immunization-induced antibodies to protect against *P. vivax* infection. The *P. vivax* blood-stage challenge model allows one to determine if a

vaccine elicits antibodies that have a biological effect to reduce parasite growth in vivo. Whether the PMR reduction of 53%[22] translates to protection against clinical disease remains to be determined. Protection against clinical *P. vivax* malaria will need to be determined in field trials in a malaria-endemic area.

In addition to binding inhibitory antibodies, ELISA recognition titres and presence of anti-PvDBPII-specific IgG1, IgG2 and IgG4 significantly contributed to PMR reduction. Consistent with our results, total IgG as well as IgG1 specific to PvDBPII SalI were associated with a reduced risk of malaria in exposed children from PNG[35]. In addition, the He et al. study[35] reported undetectable IgG3 levels for PvDBPII SalI similar to the very low levels of IgG3 detected here (Supplementary Fig. 5). However, IgG3 against PvDBPII allele AH, the most frequent allele in this region, was detected in the PNG field study[35]. IgG3 against PvDBPII allele AH was more predominant in older children and correlated with protection[35]. Other studies in malaria-endemic areas showed that there is a higher prevalence of IgG3 specific to merozoite surface proteins in *P. vivax*[36] and *P. falciparum*[37,38] with age. This evidence suggests that class-switching to antigen-specific IgG3 may develop after multiple *P. vivax* infections but not after a limited number of immunizations with PvDBPII. The IgG2 and IgG4 subclasses, which are rarely found upon natural exposure to both *P. falciparum* and *P. vivax* infections, were significant predictors of PMR reduction according to our feature selection analysis. These IgG subclasses do not bind FcγRs as efficiently as IgG1 and IgG3[39]. The immune effector mechanisms induced by anti-PvDBPII specific IgG2 and IgG4 antibodies remain to be identified.

The binding of anti-PvDBPII antibodies to FcγRs was also a significant predictor of PMR outcome. The cellular responses mediated by these receptors could play an important role in parasite growth reduction and protection against clinical symptoms as seen for *P. falciparum*. After a Phase II trial showing that vaccination with RTS,S (based on the *P. falciparum* circumsporozoite protein, PfCSP) protects against *P. falciparum* infection in malaria-naïve volunteers[40], multivariate analysis revealed that FcγRIIIa and antibody-dependent cellular phagocytosis (ADCP) were the strongest correlates of protection in a sporozoite-based CHMI[41]. Binding of anti-PfCSP antibodies to C1q was also found to correlate with RTS,S-elicited protection[41]. Largely unknown in *P. vivax*, complement-fixing antibodies of diverse blood-stage antigens in *P. falciparum* have been correlated with protection upon natural exposure[42]. Our data suggests that complement and FcγRs may also contribute to *P. vivax* growth reduction.

Importantly, Suscovich and collaborators found that IgA is a highly important predictor of RTS,S-induced protection[41]. Similarly, multivariate analysis of immune responses in a Phase I/IIa trial with blood-stage *P. falciparum* vaccine PfRH5 revealed that IgA responses were the variables with the greatest importance that contribute to PMR reduction in malaria-naïve individuals[25]. Contrary to this, our data suggest that anti-PvDBPII IgA was not a significant predictor even though it was individually correlated to PMR reduction (Supplementary Figs. 5 and 6). In addition, avidity and isotype IgM did not significantly contribute to PMR reduction. After volunteers were immunized with RTS,S and underwent CHMI, IgM was found to be a susceptibility marker for parasite infection as it was more predominant in infected volunteers[41]. In case of avidity, it also increased in malaria-naïve volunteers who received the delayed third dose of PfRH5 compared to a monthly dosing regimen[25]. We observed a similar trend of higher avidity of anti-PvDBPII antibodies in delayed dosing regimens compared to shorter dosing schedules of both vaccine platforms, groups PvDBPII/M-M (0-1-14 months) vs PvDBPII/M-M (0-1-2 months) and groups VV-PvDBPII (0-17-19 months) vs VV-PvDBPII (0–2 months). However, our feature selection algorithm showed that avidity was not an important variable for *P. vivax* PMR reduction unlike the case for anti-PfRH5 avidity and

P. falciparum[25]. In addition, two field trials analyzing the vaccine efficacy of RTS,S in children found that anti-PfCSP avidity was not statistically associated with protection[43,44].

In terms of binding kinetics of PvDBPII and anti-PvDBPII antibodies, the affinity constant, K_D, and association constant, k_a, were not selected as important by the feature selection algorithm in both datasets. Instead, the algorithm identified that the dissociation constant, k_{dis}, was a significant contributor to PMR reduction. The k_{dis} for anti-PvDBPII polyclonal antibodies indicates the stability of antibodies bound to PvDBPII. The ability of anti-PvDBPII antibodies to remain bound to PvDBPII could lead to better neutralizing and effector activities resulting in significant PMR reduction.

The data presented here identify key functional properties of PvDBPII-specific antibodies elicited by immunization that predict PMR reduction following *P. vivax* blood-stage challenge. PvDBPII-binding inhibition titres showed high importance for the prediction of PMR reduction, though other features such as antibody titre, k_{dis}, IgG1, IgG2, IgG4 and binding to C1q and FcγRs may also contribute to *P. vivax* protection.

PvDBPII/Matrix-M^TM delivered in a delayed dosing regimen has shown significant reduction in PMR. Extensive analysis of immune responses reported here has identified for the first time functional antibody immune correlates. These immune correlates together with anti-PvDBPII binding inhibition titres should be evaluated in subsequent trials and could guide the clinical development of a high-efficacy *P. vivax* vaccine based on PvDBPII.

METHODS

Study design
A full description of the Phase I/IIa clinical trial is described elsewhere[22]. Serum samples were obtained from a series of three Phase I/IIa clinical trial protocols (called VAC069, VAC071 and VAC079) conducted in parallel and designed to evaluate the efficacy of immunization with PvDBPII vaccine candidates including His-tag free recombinant PvDBPII SalI formulated with Matrix-M^TM adjuvant and viral-vectored PvDBPII SalI delivered by ChAd63 and MVA followed by blood stage challenge with the Thai *P. vivax* clinical isolate PvW1 to evaluate efficacy[22].

Expression of recombinant PvDBPII and DARC-Fc
Recombinant PvDBPII SalI (the vaccine candidate) and PvDBPII PvW1 (the binding domain of PvDBP from the *P. vivax* isolate PvW1 used for CHMI) were produced as previously described[19,45–47]. Briefly, synthetic genes encoding PvDBPII SalI and PvW1 with C-terminal 6-His tags that were codon optimized for expression in *E. coli*, were cloned into the pET28a (+) vector (GenScript) and the resultant plasmids were transformed into *E. coli* strain BL21(DE3) pLysS (C6060, Thermo Fisher). PvDBPII was expressed by fed-batch fermentation, cells were lysed, PvDBPII was solubilized from inclusion bodies under denaturing conditions and purified by nickel-charged nitrilotriacetic acid (Ni-NTA) affinity chromatography (17524802, Cytiva). Recombinant PvDBPII was refolded by rapid dilution method, dialyzed and finally purified by cation exchange (SP Sepharose column, 17115201, Cytiva) and gel filtration (Superdex 200 column) chromatography (28-9893-35, Cytiva). The final monomeric recombinant PvDBPII was stored at −80 °C.

A plasmid encoding DARC-Fc was generated by ligating the first 60 codons of human DARC (FyB allele) to sequences encoding the Fc region of human IgG1 in the mammalian expression vector pCDM8[48]. The plasmid containing the human tyrosylprotein sulfotransferase-2 (TPST-2)[48] was co-transfected with the DARC-Fc plasmid into HEK293T cells (CRL-3216, ATCC). Recombinant DARC-Fc was purified from culture supernatants by protein G

affinity chromatography. The final recombinant protein was stored at −80 °C.

ELISA

Nunc MaxiSorp ELISA plates (439454, Thermo Fisher) were coated overnight with 100μl of recombinant PvDBPII variant SalI or PvW1 proteins (1 μg/ml) in carbonate-bicarbonate buffer (C3041, Sigma) at 4 °C. Next day, plates were washed three times with 0.05% Tween (P1379, Sigma) in PBS (PBS/T) and blocked with 200 μl of 5% non-fat milk (Regilait) PBS/T for 1 h at 37 °C. Test and reference anti-PvDBPII sera (reference serum consisted of a pool of sera collected from volunteers at two weeks after the final boost in a previous PvDBPII Phase I trial[20]) were diluted in 2.5% milk (initial dilution 1:200) and 100 μl was added per well in duplicate and incubated for 1 h at 37 °C. After washing, bound antibodies were detected by adding 100 μl of horseradish peroxidase-conjugated anti-human IgG rabbit antibodies (A8792, Sigma) at dilution 1:4,000 and incubated for 1 h at 37 °C. The assay was developed at room temperature by using 100 μl of the two-component chromogenic substrate for peroxidase detection, TMB (3,3′,5,5′-tetramethylbenzidine, 5120-0047, Life Sciences), for 5 min and the reaction was stopped with 100 μl of 1 M phosphoric acid (H_3PO_4, 695017, Sigma). The optical density was measured immediately at a wavelength of 450 nm (OD_{450}). The reference serum was assigned 200 arbitrary units, AU, and the standard curve from the reference serum was used to fit a four-parameter logistic model using ADAMSEL version 3.0 software (Ed Remarque© 2021). OD_{450} values were later converted to AU using the standard curve and antibody titres of test sera were reported in AU for each sample.

Avidity

PvDBPII SalI or PvW1 pre-coated ELISA plates were incubated with test samples diluted to give an OD_{450} of ~2.0. After sample incubation, descending concentrations of the chaotropic agent sodium thiocyanate (NaSCN, 251410, Sigma) (7 M to 0 M in PBS) were added (100 μl) and incubated for 15 min at room temperature. Plates were washed with PBS/T and reaction was developed to detect bound IgGs as per ELISA protocol. OD_{450} values were plotted versus NaSCN concentration and fitted in a four-parameter logistic model. The NaSCN concentration that resulted in a 50% reduction of the OD_{450} was used as a measure of the avidity (IC_{50}).

Isotyping

PvDBPII SalI or PvW1 pre-coated ELISA plates were incubated with test samples diluted 1:100 in duplicates. After washing, the following antibodies were added for detection (100 μl at dilution 1:1,000): biotin-conjugated mouse monoclonal anti-human IgG1 (B6775, Life Technologies); biotin-conjugated mouse monoclonal anti-human IgG2 (B3398, Life Technologies); biotin-conjugated mouse monoclonal anti-human IgG3 (B3523, Sigma); biotin-conjugated mouse anti-human IgG4 (B3648, Sigma); peroxidase-conjugated goat polyclonal anti-human IgA α-chain (A0295, Sigma); and peroxidase-conjugated goat polyclonal anti-human IgM μ-chain (401905, Millipore). After 1 h incubation at 37 °C, plates were washed and avidin-peroxidase (A7419, Sigma) was added (100 μl at dilution 1:5,000), except for the IgA and IgM wells, to which 2.5% milk was added. After 1 h incubation at 37 °C, the reaction was developed like in ELISA protocol. The OD_{450} was used to evaluate the IgG subclass, IgA or IgM of each sample.

ELISA-based PvDBPII-DARC Binding Inhibition Assay

The binding of PvDBPII to DARC was analyzed in presence or absence of anti-PvDBPII antibodies using an ELISA based format as described earlier[48]. Briefly, recombinant DARC-Fc (1 μg/ml) was coated on to Nunc MaxiSorp ELISA plates overnight at 4 °C in carbonate-bicarbonate buffer. Next day, the plate was blocked for 2 h at 37 °C using 2% non-fat milk PBS/T. Recombinant PvDBPII SalI or PvW1 with concentrations in the range of 0.8–25 ng/ml (with OD_{450} of ~1 at 25 ng/ml) were used to generate the PvDBPII standard curve using a four-parameter logistic curve. Serum samples were analyzed at dilutions 1:10 to 1:2,430. Each serum dilution was incubated with 25 ng/ml PvDBPII at 37 °C for 30 min. The reaction mixture was added to wells in duplicate and incubated at 37 °C for 1 h. PvDBPII bound to DARC was probed with anti-PvDBPII polyclonal rabbit sera (generated in house) at 37 °C for 1 h and detected with peroxidase-conjugated anti-rabbit IgG secondary antibody (A6154, Sigma) at 37 °C for 1 h. The assay was developed as described in ELISA protocol. The amount of bound PvDBPII was estimated by converting OD_{450} values to protein concentrations using the PvDPBII standard curve. The interpolated protein concentration values were used to calculate percent binding (%) for each serum sample dilution. Then, the % binding inhibition for each serum dilution was calculated as follows: % Binding Inhibition = 100 - % Binding. The plot of % Binding Inhibition versus serum dilution was used to find the serum dilution at which 50% binding inhibition (IC_{50}) is achieved. Three independent replicates were averaged to determine the median IC_{50}.

Immunofluorescence assay (IFA)

A clinical isolate collected from a *P. vivax* malaria patient in Cambodia during field surveys by Institut Pasteur du Cambodge was used for IFA and PvDBPII sequence was determined by Sanger sequencing as described before[15]. An informed written consent was obtained from patient prior to enrollment. All procedures were carried out in strict accordance with relevant guidelines and regulations. The *P. vivax* clinical isolate was matured to schizont stage in culture. Schizonts were purified on Percoll and used to prepare slides for use in immunofluorescence assays. Slides were fixed and frozen at −70 °C in presence of desiccant. Frozen slides of *P. vivax* schizonts were thawed at room temperature for 30 min. Slides were blocked with 5% bovine serum albumin (BSA, A7030, Sigma) in PBS for 30 min at 37 °C and probed with test sera diluted in 2.5% BSA at 1:200, 1:500 and 1:5,000 for 30 min at 37 °C, followed by three washes with PBS. A mixture of Alexa Flour 488-conjugated goat anti-human IgG (H + L) secondary antibodies (A11013, Themo Fisher) at 1:500 and Hoeschst 33342 solution (62249, Thermo Fisher) at 1:20,000 was added and incubated for 30 min at 37 °C. After washing, slides were treated with anti-Fade (H-1000-10, Vector Laboratories) and visualized on Leica DM 5000B Microscope (Leica Microsystems). The fluorescence intensity of each sample was scored as follows: +++, for high intensity; ++, medium intensity; +, low intensity; and -, no signal.

Antibody affinity by biolayer interferometry (BLI)

Experiments were performed on an Octet RED 384 instrument (Fortebio) at 25 °C with shaking at 1,000 round per minute (rpm). All assays were conducted in standard Greiner black 96-well microtiter plates (655209, Greiner) in a volume of 120 μl/well. Buffer consisting of PBS with 1 mg/ml BSA was used for baselines, dissociation steps and to dilute recombinant proteins. Sera were diluted in PBS to achieve final concentrations of IgGs in the range of 30 to 0 nM. This optimal range gives a sensogram with even spacing between the binding signals at different concentrations. The method was set as follows: NTA biosensors (18-5101, Sartorius) were hydrated for 10 min in PBS and regenerated (3 cycles, 30 s each) with 10 mM glycine pH 1.5 (410225, Sigma), followed by another regeneration with 50 mM ethylenediamine-tetraacetic acid (EDTA) (EDS, Sigma). Biosensors were activated with 10 mM nickel sulfate ($NiSO_4$, 656895, Sigma) for 180 s and later dipped in buffer (120 s). PvDBPII variant SalI or PvDBPII PvW1

were immobilized via His tag at 5 µg/ml for 600 s. A mammalian cytosolic protein, peroxiredoxin 6 (PRDX6)[49], was loaded at 3 µg/ml to pre-charged NTA biosensors for 600 s as a reference biosensor (negative control). Loaded biosensors were tested for binding to test sera in the following steps: baseline (60 s in buffer), association step (600 s in serum dilutions) and dissociation step (600 s in buffer). Two wells containing only buffer instead of sera were assigned as reference wells. Signals from reference wells and reference biosensors were later subtracted. Affinity, association and dissociation constants (K_D, k_a and k_{dis}, respectively) were calculated by Data Analysis HT software version 10 (Fortebio) using kinetic analysis and a 1:1 binding model.

Binding analysis to complement component C1q and Fc receptors by BLI

Experiments were performed on an Octet HTX instrument (Fortebio) at 25 °C with shaking at 1,000 rpm. All assays were conducted in standard black 384-well microtiter plates (781209, Greiner) and volume was 120 µl/well. The following recombinant proteins diluted in PBS containing 1 mg/ml BSA (PBS-BSA) were used to determine binding to sera: C1q (ab282858, Abcam) at 12 nM; the Fc gamma receptor (FcγR) Ia (FcγRIa), FcγRIIa, FcγRIIb, and FcγRIIIa (all from Sino Biological: 10256-H08H, 10374-H08H1, 10259-H08H and 10389-H08H1, respectively) at dilutions 19 nM, 1.7 µM, 3.7 µM and 2.3 µM, respectively. The method was set as follows, including the reagents from the AR2G Reagent kit (18-5095, Sartorius): Amine-reactive second-generation (AR2G) biosensors (18-5092, Sartorius) were activated as per manufacturer's protocol in 20 mM 1-Ethyl-3-(3-Dimethylamino propyl) Carbodiimide, hydrochloride (EDC) and 10 mM sulfo N-hydroxysuccinimide (s-NHS) solution for 300 s. PvDBPII SalI domain, PvDBPII PvW1 recombinant protein or PRDX6 (reference biosensor) were immobilized at 20 µg/ml in 10 mM acetate buffer pH 6 for 600 s. Loaded biosensors were quenched with 1 M ethanolamine pH 8.5 for 300 s. Later, biosensors were regenerated (3 cycles, 30 s each) with 10 mM glycine pH 1.5 and dipped into wells containing serum diluted in PBS-BSA at 1:100 for 600 s. After an incubation of 900 s in PBS-BSA to stabilize the signals, biosensors were tested for binding to C1q and FcγRs in the following steps: baseline (120 s in PBS-BSA), association step (600 s in C1q and FcγR dilutions) and dissociation step (600 s in PBS-BSA). Wells containing PBS-BSA alone were assigned as reference wells. Signals from reference wells and reference biosensors were later subtracted. Binding to C1q and FcγRs was measured as the wavelength shift signal or response (nm) at the end of the association step. All the data were analyzed using Octet BLI Analysis Studio 13.0 software.

Statistics

Because of the complex structure of the data, we used frequently-used statistical tests for analysis of univariate data, and machine learning algorithms for analysis of multivariate data. Comparisons among vaccinated groups and timepoints in antibody and binding inhibition titres were performed using a Kruskal–Wallis test with Dunn's correction for multiple comparisons. Differences between SalI and PvW1 were tested with pairwise comparisons with Bonferroni's multiple comparison tests. Correlations between variables were determined by Spearman rank test. All statistical tests were two-sided and a p value < 0.05 was considered significant. Modeling of PMR reduction including only the binding inhibition titres specific to both PvDBPII alleles was performed by Random Forest regression. Data analysis and graphs were performed using GraphPad Prism version 9.3.1 (GraphPad Software Inc.). The correlation plot of all variables and Random Forest regression were generated in R version 4.2.2 and RStudio version 2022.12.0 + 353.

Feature selection was performed using a Boruta algorithm[24,50]. The Boruta algorithm is a wrapper method built around a random forest classifier that performs a top-down search for relevant features, while progressively eliminating irrelevant features, by comparing the importance of original features with the importance achievable at random (shadow features, estimated using permuted copies of the original features). To measure the importance of the immunological readouts that significantly contribute to the PMR outcome, we applied the Boruta algorithm using R version 4.2.2 and RStudio version 2022.12.0 + 353.

Ethics Statement

Sera from volunteers participating in the three clinical trials conducted at the University of Oxford, UK were sent to Institut Pasteur, Paris under a Material Transfer Agreement. The clinical trial studies had received ethical approval from UK National Health Service Research Ethics Services, (VAC069: Hampshire A Research Ethics Committee, Ref 18/SC/0577; VAC071: Oxford A Research Ethics Committee, Ref 19/SC/0193; VAC079: Oxford A Research Ethics Committee, Ref 19/SC/0330). The vaccine trials were approved by the UK Medicines and Healthcare products Regulatory Agency (VAC071: EudraCT 2019-000643-27; VAC079: EudraCT 2019-002872-14). The trials are registered under the following ClinicalTrials.gov numbers: VAC069 NCT03797989, VAC071 NCT04009096, VAC079 NCT04201431. The research conducted at the Institut Pasteur received approval from the Institutional Review Board (IRB) of the Institut Pasteur (Research Ref IRB2022-03).

Reporting summary

Further information on research design is available in the Nature Research Reporting Summary linked to this article.

DATA AVAILABILITY

The datasets used and/or analyzed during this study are available upon reasonable request made to the corresponding author.

CODE AVAILABILITY

The underlying code for this study is not available publicly but will be made available by the corresponding author to researchers on reasonable request.

REFERENCES

1. World Health Organization. World malaria report 2022. (2022).
2. Baird, J. K. Evidence and Implications of Mortality Associated with Acute Plasmodium vivax Malaria. Clin. Microbiol. Rev. **26**, 36–57 (2013).
3. Rahimi, B. A. et al. Severe vivax malaria: a systematic review and meta-analysis of clinical studies since 1900. Malar. J. **13**, 481 (2014).
4. Mueller, I. et al. Key gaps in the knowledge of Plasmodium vivax, a neglected human malaria parasite. Lancet Infect. Dis. **9**, 555–566 (2009).
5. Robinson, L. J. et al. Strategies for Understanding and Reducing the Plasmodium vivax and Plasmodium ovale Hypnozoite Reservoir in Papua New Guinean Children: A Randomised Placebo-Controlled Trial and Mathematical Model. PLoS Med **12**, e1001891 (2015).
6. McKenzie, F. E. et al. Gametocytemia in Plasmodium vivax and Plasmodium falciparum infections. J. Parasitol. **92**, 1281–1285 (2006).
7. Miller, L. H., Mason, S. J., Clyde, D. F. & McGinniss, M. H. The Resistance Factor to Plasmodium vivax in Blacks — The Duffy-Blood-Group Genotype, FyFy. N. Engl. J. Med. **295**, 302–304 (1976).
8. Horuk, R. et al. A Receptor for the Malarial Parasite Plasmodium vivax: the Erythrocyte Chemokine Receptor. Science **261**, 1182–1184 (1993).
9. Chitnis, C. E. & Miller, L. H. Identification of the Erythrocyte Binding Domains of Plasmodium vivax and Plasmodium knowlesi Proteins Involved in Erythrocyte Invasion. J. Exp. Med. **180**, 497–506 (1994).
10. Xainli, J., Adams, J. H. & King, C. L. The erythrocyte binding motif of Plasmodium vivax Duffy binding protein is highly polymorphic and functionally conserved in isolates from Papua New Guinea. Mol. Biochem. Parasitol. **111**, 253–260 (2000).

11. Kho, W.-G., Chung, J.-Y., Sim, E.-J., Kim, D.-W. & Chung, W.-C. Analysis of polymorphic regions of *Plasmodium vivax* Duffy binding protein of Korean isolates. *Korean J. Parasitol.* **39**, 143 (2001).

12. Gosi, P. et al. Polymorphism patterns in Duffy-binding protein among Thai *Plasmodium vivax* isolates. *Malar. J.* **7**, 112 (2008).

13. Hans, D. et al. Mapping binding residues in the *Plasmodium vivax* domain that binds Duffy antigen during red cell invasion: Binding residues of *P. vivax* Duffy binding protein. *Mol. Microbiol.* **55**, 1423–1434 (2005).

14. Singh, S. K., Hora, R., Belrhali, H., Chitnis, C. E. & Sharma, A. Structural basis for Duffy recognition by the malaria parasite Duffy-binding-like domain. *Nature* **439**, 741–744 (2006).

15. Roesch, C. et al. Genetic diversity in two *Plasmodium vivax* protein ligands for reticulocyte invasion. *PLoS Negl. Trop. Dis.* **12**, e0006555 (2018).

16. King, C. L. et al. Naturally acquired Duffy-binding protein-specific binding inhibitory antibodies confer protection from blood-stage *Plasmodium vivax* infection. *PNAS* **105**, 8363–8368 (2008).

17. Nicolete, V. C., Frischmann, S., Barbosa, S., King, C. L. & Ferreira, M. U. Naturally Acquired Binding-Inhibitory Antibodies to *Plasmodium vivax* Duffy Binding Protein and Clinical Immunity to Malaria in Rural Amazonians. *J. Infect. Dis.* **214**, 1539–1546 (2016).

18. Wiley, S. R. et al. Targeting TLRs Expands the Antibody Repertoire in Response to a Malaria Vaccine. *Sci. Transl. Med.* **3**, (2011).

19. Bhardwaj, R. et al. Production of recombinant PvDBPII, receptor binding domain of *Plasmodium vivax* Duffy binding protein, and evaluation of immunogenicity to identify an adjuvant formulation for vaccine development. *Protein Expr. Purif.* **136**, 52–57 (2017).

20. Singh, K. et al. Malaria vaccine candidate based on Duffy-binding protein elicits strain transcending functional antibodies in a Phase I trial. *npj Vacc* **3**, 48 (2018).

21. Payne, R. O. et al. Human vaccination against *Plasmodium vivax* Duffy-binding protein induces strain-transcending antibodies. *JCI Insight* **2**, e93683 (2017).

22. Hou, M. M. et al. Vaccination with *Plasmodium vivax* Duffy-binding protein inhibits parasite growth during controlled human malaria infection. *Sci. Transl. Med.* **15**, eadf1782 (2023).

23. Minassian, A. M. et al. Controlled human malaria infection with a clone of *Plasmodium vivax* with high-quality genome assembly. *JCI Insight* **6**, e152465 (2021).

24. Kursa, M. B. & Rudnicki, W. R. Feature Selection with the Boruta Package. *J. Stat. Soft.* **36**, (2010).

25. Minassian, A. M. et al. Reduced blood-stage malaria growth and immune correlates in humans following RH5 vaccination. *Med* **2**, 701–719.e19 (2021).

26. Nielsen, C. M. et al. Delayed boosting improves human antigen-specific Ig and B cell responses to the RH5.1/AS01B malaria vaccine. *JCI Insight* **8**, e163859 (2023).

27. Flaxman, A. et al. Reactogenicity and immunogenicity after a late second dose or a third dose of ChAdOx1 nCoV-19 in the UK: a substudy of two randomised controlled trials (COV001 and COV002). *Lancet* **398**, 981–990 (2021).

28. Parry, H. et al. Extended interval BNT162b2 vaccination enhances peak antibody generation. *npj Vaccines* **7**, 14 (2022).

29. Barrett, J. et al. Analyses of vaccine-specific circulating and bone marrow-resident B cell populations reveal benefit of delayed vaccine booster dosing with blood-stage malaria antigens. *medRxiv* (2023) https://doi.org/10.1101/2023.03.17.23287040.

30. Lawrence, G. et al. Effect of vaccination with 3 recombinant asexual-stage malaria antigens on initial growth rates of Plasmodium falciparum in non-immune volunteers. (2000).

31. Spring, M. D. et al. Phase 1/2a Study of the Malaria Vaccine Candidate Apical Membrane Antigen-1 (AMA-1) Administered in Adjuvant System AS01B or AS02A. *PLoS one* **4**, e5254 (2009).

32. Sheehy, S. H. et al. ChAd63-MVA–vectored Blood-stage Malaria Vaccines Targeting MSP1 and AMA1: Assessment of Efficacy Against Mosquito Bite Challenge in Humans. *Mol. Ther.* **20**, 2355–2368 (2012).

33. Payne, R. O. et al. Demonstration of the Blood-Stage *Plasmodium falciparum* Controlled Human Malaria Infection Model to Assess Efficacy of the *P. falciparum* Apical Membrane Antigen 1 Vaccine, FMP2.1/AS01. *J. Infect. Dis.* **213**, 1743–1751 (2016).

34. Dejon-Agobe, J. C. et al. Controlled Human Malaria Infection of Healthy Adults With Lifelong Malaria Exposure to Assess Safety, Immunogenicity, and Efficacy of the Asexual Blood Stage Malaria Vaccine Candidate GMZ2. *Clin. Infect. Dis.* **69**, 1377–1384 (2019).

35. He, W.-Q. et al. Antibody responses to *Plasmodium vivax* Duffy binding and Erythrocyte binding proteins predict risk of infection and are associated with protection from clinical Malaria. *PLoS Negl. Trop. Dis.* **13**, e0006987 (2019).

36. Oyong, D. A. et al. Induction and Kinetics of Complement-Fixing Antibodies Against *Plasmodium vivax* Merozoite Surface Protein 3α and Relationship With Immunoglobulin G Subclasses and Immunoglobulin M. *J. Infect. Dis.* **220**, 1950–1961 (2019).

37. Tongren, J. E. et al. Target Antigen, Age, and Duration of Antigen Exposure Independently Regulate Immunoglobulin G Subclass Switching in Malaria. *Infect. Immun.* **74**, 257–264 (2006).

38. Stanisic, D. I. et al. Immunoglobulin G Subclass-Specific Responses against *Plasmodium falciparum* Merozoite Antigens Are Associated with Control of Parasitemia and Protection from Symptomatic Illness. *Infect. Immun.* **77**, 1165–1174 (2009).

39. Bruhns, P. et al. Specificity and affinity of human Fc gamma receptors and their polymorphic variants for human IgG subclasses. *Am. J. Hematol.* **113**, 10 (2009).

40. Ockenhouse, C. F. et al. Ad35.CS.01 - RTS,S/AS01 Heterologous Prime Boost Vaccine Efficacy against Sporozoite Challenge in Healthy Malaria-Naïve Adults. *PLoS one* **10**, e0131571 (2015).

41. Suscovich, T. J. et al. Mapping functional humoral correlates of protection against malaria challenge following RTS,S/AS01 vaccination. *Sci. Transl. Med.* **12**, eabb4757 (2020).

42. Reiling, L. et al. Targets of complement-fixing antibodies in protective immunity against malaria in children. *Nat. Commun.* **10**, 610 (2019).

43. Olotu, A. et al. Avidity of Anti-Circumsporozoite Antibodies following Vaccination with RTS,S/AS01E in Young Children. *PLoS one* **9**, e115126 (2014).

44. Ajua, A. et al. The effect of immunization schedule with the malaria vaccine candidate RTS,S/AS01E on protective efficacy and anti-circumsporozoite protein antibody avidity in African infants. *Malar. J.* **14**, 72 (2015).

45. Singh, S. et al. Biochemical, Biophysical, and Functional Characterization of Bacterially Expressed and Refolded Receptor Binding Domain of *Plasmodium vivax* Duffy-binding. *Protein J. Bio. Chem.* **276**, 17111–17116 (2001).

46. Yazdani, S. S., Shakri, A. R., Mukherjee, P., Baniwal, S. K. & Chitnis, C. E. Evaluation of immune responses elicited in mice against a recombinant malaria vaccine based on *Plasmodium vivax* Duffy binding protein. *Vaccine* **22**, 3727–3737 (2004).

47. Yazdani, S. S., Shakri, A. R., Pattnaik, P., Rizvi, M. M. A. & Chitnis, C. E. Improvement in Yield and Purity of a Recombinant Malaria Vaccine Candidate Based on the Receptor-Binding Domain of *Plasmodium vivax* Duffy Binding Protein by Codon Optimization. *Biotechnol. Lett.* **28**, 1109–1114 (2006).

48. Shakri, A. R., Rizvi, M. M. A. & Chitnis, C. E. Development of quantitative receptor-ligand binding assay for use as a tool to estimate immune responses against *Plasmodium vivax* Duffy binding protein region II. *J. Immunoass.* **33**, 403–413 (2012).

49. Wagner, M. P. et al. Human peroxiredoxin 6 is essential for malaria parasites and provides a host-based drug target. *Cell Rep.* **39**, 110923 (2022).

50. Yman, V. et al. Distinct kinetics of antibodies to 111 *Plasmodium falciparum* proteins identifies markers of recent malaria exposure. *Nat. Commun.* **13**, 331 (2022).

ACKNOWLEDGEMENTS

AUTHOR CONTRIBUTIONS

F.J.M. expressed recombinant proteins, performed assays, analyzed data and wrote the manuscript. M.W. analyzed data. M.G.B. performed immuno-assays. C.H. expressed recombinant proteins. A.B., F.A. and P.E. reviewed data. JP provided samples. M.M.H., S.E.S., J.R.B., C.M.N. generated and provided samples. J.M.R. provided Matrix-M™ adjuvant. P.M. and V.S.C. supported vaccine development, production and project management. A.M.M. and S.J.D. were investigators on the clinical trial. C.E.C. developed the PvDBPII/Matrix M vaccine, designed the study, analyzed the

data and wrote the manuscript. All authors reviewed the manuscript and agreed with the final version.

COMPETING INTERESTS

ADDITIONAL INFORMATION